DOI: 10.21122/2220-9506-2025-16-4-306-314

A Concept of an Integral Optical Pressure Sensor

E.S. Barbin[1], P.F. Baranov[2], D.P. Ilyaschenko[2], T.G. Nesterenko[1,2], S.E. Vtorushin[1], A.A. Talovskaya[1]

[1]Tomsk State University of Control Systems and Radioelectronics,
Lenin Ave., 40, Tomsk 634034, Russia
[2]National Research Tomsk Polytechnic University,
Lenin Ave., 30, Tomsk 634050, Russia

Received 06.10.2025
Accepted for publication 01.12.2025

Abstract

Today, an expanding application of automatic systems demands research and development of novel types of sensors suitable for special conditions. Specifically, microelectromechanical pressure sensors are among of the most widely implemented devices. A pressure sensor comprises a silicon membrane that deforms under pressure of the medium and a measuring transducer that converts the deformation into electrical signal. The most promising and technologically advanced type of transducers for microelectromechanical pressure sensors are evanescent coupling-based transducers that implement light intensity passing through the gap between two optical waveguides varying under membrane deformation. Such scheme provides high sensitivity and extended dynamic range of the sensor. The paper is aimed at developing a design concept for the sensing element of a microelectromechanical pressure sensor with an evanescent coupling-based transducer. The technology for micro-optoelectromechanical sensor fabrication bases on a stepwise formation of the structures on two silicon on insulator wafers with their consequent bonding. The membrane is formed on the bottom wafer. The top wafer comprises stoppers. The waveguide structures are formed on both the wafers. We consider two methods of waveguide fabrication. First, they can be built up from silicon nitride by plasma-enhanced chemical vapor deposition. Second, they can be etched directly in the silicon wafer. The main characteristics of the pressure sensor are determined: losses, dependencies of the transmission coefficients on the length and width of the waveguides, gap, coupling length. The working range, where the optical transducer can measure membrane displacements proportional to the acting pressure reached 500±80 nm for the silicon on insulator waveguide and 600±80 nm for the Si_3N_4 waveguide. The optical transmission coefficient ranges from 0 to 0.86 for the silicon on insulator waveguide and from 0.09 to 0.53 for the Si_3N_4 waveguide. The main requirement to the membrane is assumed that its deformation does not exceed 80 nm.

Keywords: pressure sensor, optical waveguides, directional coupler

Адрес для переписки:
Ильященко Д.П.
Национальный исследовательский Томский политехнический университет,
пр-т Ленина, 30, г. Томск 634050, Россия
e-mail: mita8@tpu.ru

Address for correspondence:
Il'yaschenko D.P.
National Research Tomsk Polytechnic University,
Lenin Ave., 30, Tomsk 634050, Russia
e-mail: mita8@tpu.ru

Для цитирования:
Е.С. Барбин, П.Ф. Баранов, Д.П. Ильященко, Т.Г. Нестеренко, С.Е. Вторушин, А.А. Таловская.
Концепция построения интегрального оптического датчика давления.
Приборы и методы измерений.
2025. Т. 16. № 4. С. 306-314.
DOI: 10.21122/2220-9506-2025-16-4-306-314

For citation:
Barbin ES, Baranov PF, Ilyaschenko DP, Nesterenko TG, Vtorushin SE, Talovskaya AA.
A Concept of an Integral Optical Pressure Sensor.
Devices and Methods of Measurements.
2025;16(4):306-314.
DOI: 10.21122/2220-9506-2025-16-4-306-314

DOI: 10.21122/2220-9506-2025-16-4-306-314

Концепция построения интегрального оптического датчика давления

Е.С. Барбин[1], П.Ф. Баранов[2], Д.П. Ильященко[2], Т.Г. Нестеренко[1,2], С.Е. Вторушин[1], А.А. Таловская[1]

[1]Томский государственный университет систем управления и радиоэлектроники, пр-т Ленина, 40, г. Томск 634034, Россия

[2]Национальный исследовательский Томский политехнический университет, пр-т Ленина, 30, г. Томск 634050, Россия

Поступила 06.10.2025
Принята к печати 01.12.2025

Расширение области применения автоматизированных систем требует разработки и исследований новых типов датчиков, способных работать в специальных условиях. Одними из распространённых сенсоров являются микроэлектромеханические датчики давления. Датчик давления содержит мембрану из кремния, которая деформируется при приложении к ней давления среды, и измерительный преобразователь деформации в электрический сигнал. Наиболее перспективным и технологичным интегральным типом преобразователя для микроэлектромеханических датчиков давления является измерительный преобразователь на основе эффекта оптического туннелирования, который основан на изменении интенсивности света, проходящего через зазор между двумя оптическими волноводами при деформации мембраны, что обеспечивает высокую чувствительность и широкий динамический диапазон датчика. Целью работы являлась разработка концепции построения чувствительного элемента микроэлектромеханического датчика давления с оптическим туннельным преобразователем. Технология создания микрооптоэлектромеханического датчика давления представляет собой поэтапное формирования заданных структур на двух пластинах с последующим их соединением. На нижней пластине формируется мембрана и волноводные структуры, на верхней – стопперы и волноводные структуры. Рассмотрено два варианта выполнения волноводов: из нитрида кремния методом плазмохимического осаждения или из кремния на готовой SOI платине. Определены основные характеристики (потери, зависимости коэффициентов передачи от длины и ширины волноводов, зазора, длины связи) датчика давления. Рабочий участок, на котором оптический датчик может измерять перемещения мембраны, пропорциональные действующему давлению, лежит в пределах от 500±80 нм для SOI, и 600±80 нм для Si_3N_4. Оптический коэффициент передачи меняется в диапазоне от 0 до 0,86 для SOI и от 0,09 до 0,53 для Si_3N_4, соответственно. Требованием к мембране можно считать, что её деформация во всем диапазоне давлений должна лежать в диапазоне до 80 нм.

Ключевые слова: датчик давления, оптические волноводы, направленный ответвитель

Адрес для переписки:
Ильященко Д.П.
Национальный исследовательский Томский политехнический университет,
пр-т Ленина, 30, г. Томск 634050, Россия
e-mail: mita8@tpu.ru

Address for correspondence:
Il'yaschenko D.P.
National Research Tomsk Polytechnic University,
Lenin Ave., 30, Tomsk 634050, Russia
e-mail: mita8@tpu.ru

Для цитирования:
Е.С. Барбин, П.Ф. Баранов, Д.П. Ильященко, Т.Г. Нестеренко, С.Е. Вторушин, А.А. Таловская.
Концепция построения интегрального оптического датчика давления.
Приборы и методы измерений.
2025. Т. 16. № 4. С. 306-314.
DOI: 10.21122/2220-9506-2025-16-4-306-314

For citation:
Barbin ES, Baranov PF, Ilyaschenko DP, Nesterenko TG, Vtorushin SE, Talovskaya AA.
Laser Speckle Correlation Method in Diagnostics of Bridge Span Vibrations.
Devices and Methods of Measurements.
2025;16(4):306-314.
DOI: 10.21122/2220-9506-2025-16-4-306-314

Introduction

As of today, an expanding application of automatic systems demands the research and development of novel types of sensors suitable for specific conditions and fields, including areas with explosion and fire hazard, elevated or low temperatures, increased radiation levels, strong electromagnetic fields, and invasive/non-invasive medicine as well. Among the most commonly used are pressure sensors. Microelectromechanical (MEMS) pressure sensors are used in the oil and gas and automotive industries, control systems of space vehicles and launch site ground facilities, in steam and gas turbines to control pressure fluctuations and measure dynamic pressure at high temperatures, in atomic reactors, personalized medicine or smart home systems. Increased accuracy and sensitivity of pressure sensors (capability of detecting small pressure fluctuations) allow for early identification of industrial and natural emergency situations.

The working principles of the majority of microelectronic pressure sensors are based on the membrane deformation under measured pressure that can be detected as an electrical signal using various measuring transducers. Depending on the application field, the sensors can be capacitive, piezoelectric, tensoresistive and of other types described elsewhere [1–3]. The said pressure measurement mechanisms determine the required characteristics of the device, such as measured pressure range, accuracy, non-linearity, sensitivity, etc.

The capacitive measuring transducers are a compromise between the working range and sensitivity due to an incorporated feedback system and cover the overwhelming majority of market demands in various application spheres. However, the resolution and minimal sensitivity threshold of such sensors is mainly limited by their design concept [4–7]. The sensor's capability to detect displacements, that in capacitive terms correspond to units of femtofarads is limited by the noise threshold of electronic components and, to larger extent, by stray capacitances inside the sensor. To compensate the destabilizing factors (capacitive couplings, temperature, electromagnetic impacts, etc.), complex design and fabrication approaches are used. An ideal option is to arrange all the electronic components immediately in a single package with the MEMS transducer.

In terms of elimination of the above-mentioned drawbacks, the most promising types of measuring transducers are tenso- and piezoresistive [8–11], resonant, optical and piezoelectric [12] systems.

Piezoelectric MEMS pressure sensors [12] possess the following advantages: small weight, high reliability, simple design, high signal-to-noise ratio, high sensitivity and bandwidth, fast signal change response, resistance to shock impacts and vibrations, low hysteresis effects, capability to measure the pressure in various aggressive media. However, some piezoelectric materials require hydroprotection, implementation of a charge amplifier or a scheme with high input resistance. They are also inapplicable to measure static pressure. To reduce the sensor's dimensions while retaining high accuracy, the piezoelectric MEMS pressure sensor should be fabricated using thin-film technologies, which would enable its application in invasive and non-invasive medicine.

The resonant sensors [13–17] provide high measuring accuracy in extreme operating conditions. Thanks to absolute elastic properties of monocrystalline silicon, it has no hysteresis (<0.001 % of measured value) and is almost perfectly linear (<0.003 % of measured value). The eigenfrequencies of the resonators are far beyond the spectrum of industrial noise, which makes them immune to vibrations. The resonance sensor lacks drift factors, because monocrystalline silicon is chemically inert and exhibits no fatigue, which ensures is nearly absolute stability. The frequency output signal of the sensor requires no analog-to-digital conversion. However, the only manufacturer of such transducers is Yokogawa Electric Corporation (Japan).

Another promising type of transducers are optical pressure sensors [18–22]. The most investigated and marketed among them are optical fiber sensors implementing fiber Bragg gratings. Sensors based on fiber Bragg gratings have high noise resistance, fire safety and small dimensions. This is conditioned by the fact that optical signal modulation requires small exposure on the section with the Bragg grating, irrespective of it to be mechanical or thermal. However, this induces major impediments to the application of Bragg grating-based transducers in high-precision measurements. They require a special case that transmits measured pressure to the optical fiber section with the grating and either protects it from thermal impact, or contains an additional temperature sensor for consequent correction of the measured pressure value. Moreover, they need expensive equipment to ensure accurate and fast processing of initial and reflected light signals. This increases the mass and dimensions of both sensor and necessary equipment. Therefore, further miniaturization and cost reduction of optical pressure sensor fabrication require novel types of transducers possessing the advantages of optical methods, while lacking some of their drawbacks.

Over the recent years, the development of micro- and nanoelectronics has induced increasing interest in the field of photonic integrated schemes. The most promising and technologically advanced integrated type of transducers for pressure sensors are evanescent coupling-based systems that possess lower thermal sensitivity and require no complex output signal processing scheme or expensive equip ment [23].

In world literature, the research works on integrated optical methods applied to pressure sensors are scarce. However, it is beyond a doubt that schemes based on optical transducers considerably overpass conventional schemes and are suitable for mass production. The technological elaboration of integrated optical waveguide coupling with movable microelectromechanical structures is to be investigated as well. Therefore, such research works are valuable on both fundamental and practical levels.

This treatise is aimed at investigating a novel type of the measuring transducer of a MEMS pressure sensor based on evanescent coupling. This makes feasible a pressure sensor with not only remote light input to and output from the measured object through optical fiber. Moreover, such scheme allows for integrated packaging of the sensor's components (electronics, laser and photodiode) in a single case, which vastly expands the application field of such measuring transducers.

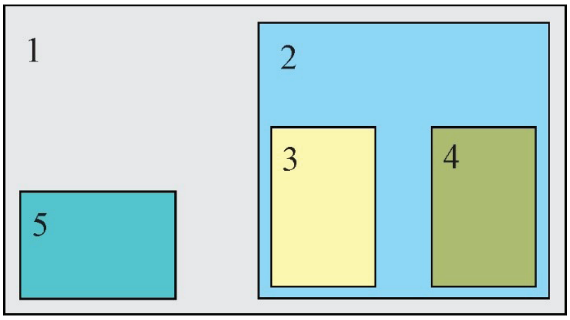

Figure 1 – Pressure sensor design: 1 – pressure sensor; 2 – sensing element; 3 – membrane; 4 – measuring transducer; 5 – electronic box

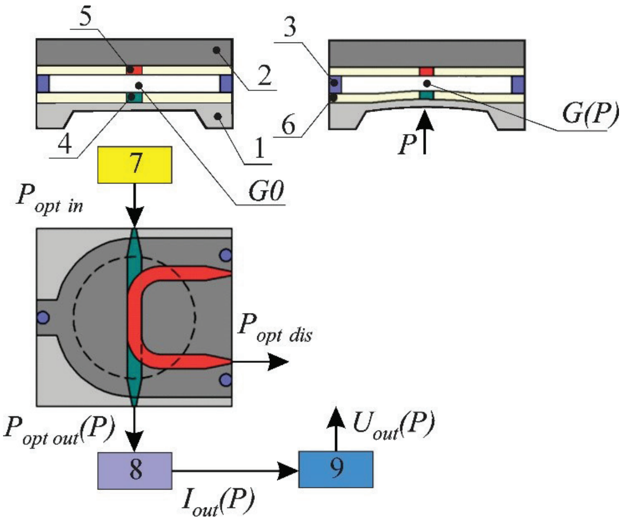

Figure 2 – Functional scheme of the pressure sensor: 1 – bottom wafer; 2 – top wafer; 3 – G_0 stopper; 4 – bottom integrated waveguide; 5 – top integrated waveguide; 6 – SiO_2 layer; 7 – laser diode; 8 – photodiode; 9 – electronic box

Pressure sensor design

Functional scheme

The pressure sensor (Figure 1) comprises an electronic box (EB) for data processing and power supply. The sensing element consists of a membrane and a measuring transducer. The membrane converts applied pressure into displacement, while the measuring transducer converts the membrane displacement into another form of data (current, voltage, frequency, etc.) that is fed to the EB.

Integrated optical pressure sensor is an micro-optoelectromechanical system which functional scheme is given in Figure 2.

The sensing element of the micro-optoelectromechanical (MOEM) pressure sensor contains bottom wafer with membrane 1 and top wafer 2 coupled by stoppers 3 intended for the formation of initial air gap G_0. Both wafers comprise bottom 4 and top 5 optical integrated waveguides surrounded by silicon oxide layers 6. Optical waveguides 4 and 5 form the optical measuring transducer (OMT) implemented as a directional coupler. Optical radiation from a laser diode 7 is fed into bottom waveguide 4 with optical power $P_{opt\ in}$, that at working gap G_0 flows into top waveguide 5 with power $P_{opt\ diss} = 0.5 \cdot P_{opt\ in}$ and consequently dissipates. The output optical signal from the sensing element of the MOEM pressure sensor hits a photodiode 8 with power $P_{opt\ out}(P)$

at which output signal $I_{out\ put}$ (P) forms that is then amplified by the EB 9 and consequently transformed into voltage. Under pressure P, membrane bends, thus changing gap $G(P)$ between waveguides 4 and 5 of the OMT. This alters the optical power at the output of the bottom waveguide $I_{out\ put}$ (P) proportionally to the membrane bend and, respectively, applied pressure.

Technological process

The technology for microoptoelectromechanical sensor fabrication lies in the stepwise formation of structures on two silicon on insulator (SOI) wafers with their consequent bonding. The membrane is formed on the bottom wafer. The top wafer comprises stoppers. The waveguide structures are formed on both the wafers (Figure 3).

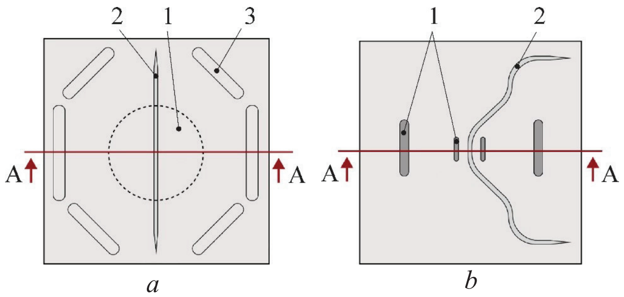

Figure 3 – Wafers of the micro-optoelectromechanical pressure sensor: *a* – bottom wafer (1 – pressure application area, 2 – waveguide, 3 – air channel); *b* – top wafer (1 – stopper, 2 – waveguide)

The first step of pressure sensor membrane formation involves the application of a protective mask on the silicon wafer surface by etching the dielectric through a photoresistive mask. Then, liquid or plasma-enhanced chemical etching of silicon is performed with further removal of the protective mask (Figure 4).

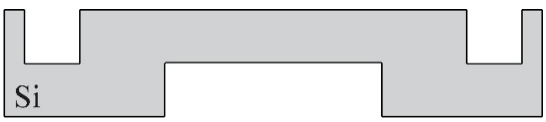

Figure 4 – First silicon wafer after membrane formation

The waveguide structures are formed identically for both wafers. First, a stepwise plasma-enhanced chemical vapor deposition of SiO_2 and Si_3N_4 is performed. Then, waveguide structures are formed in the silicon nitride layer by plasma-enhanced chemical etching along the photoresistive mask (Figure 5).

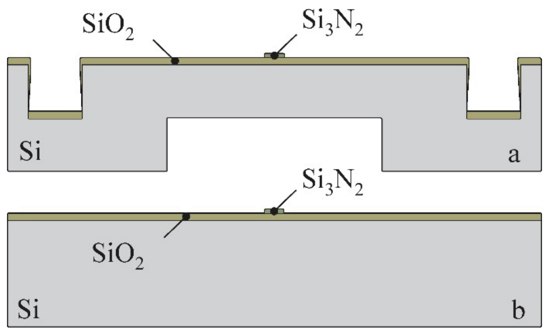

Figure 5 – Wafer after waveguide formation: *a* – bottom wafer; *b* – top wafer

After that, stoppers are formed on the second wafer by electron-beam sputtering of aluminum oxide along a two-layer photoresistive mask with its consequent removal (explosion) in an organic solvent. First, stoppers are built up that prevent the contact of the two waveguides at critical loads. Then, the stoppers forming the initial air gap are built up (Figure 6).

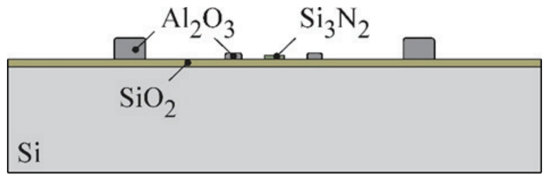

Figure 6 – Second silicon wafer after stoppers buildup

The final step in MOEM pressure sensor fabrication is the adjustment and bonding of the wafers by an adhesive (Figure 7).

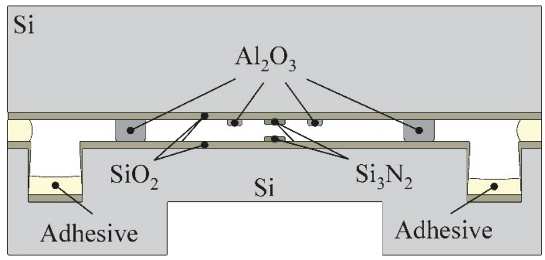

Figure 7 – Scheme of the micro-optoelectromechanical pressure sensor

Geometric parameters of waveguide

The waveguides can be fabricated from silicon nitride by plasma-enhanced chemical vapor deposition or from silicon directly in the SOI wafer. Following the principle of minimal losses, let us select height h and width w of a single waveguide from Si_3N_4 by the mode overlap method (Figure 8).

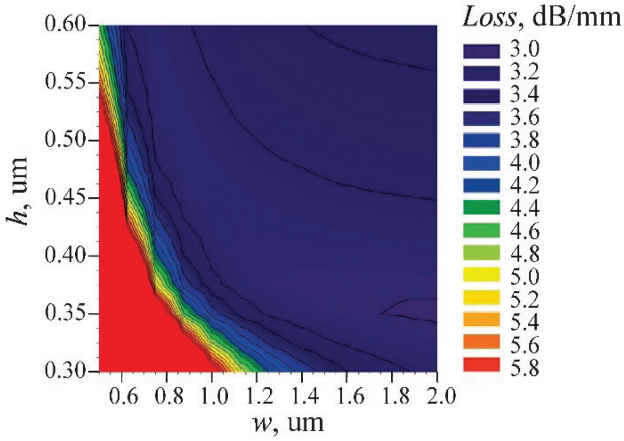

Figure 8 – Losses in the waveguide depending on the height and width of the waveguides

The width of the waveguides can be increased while increasing their height. Following the technology of silicon nitride film deposition, the layer's height should be decreased to prevent cracking of the films and reduce internal stresses after deposition. The cracking can occur at a height exceeding 400 nm. Therefore, in further research we used a height of the Si_3N_4 layer of 350 nm. The increased width of the waveguide lowered the losses: the minimum value was observed at a width beyond 1.2 um and amounted to 2.8 dB/mm (Figure 9).

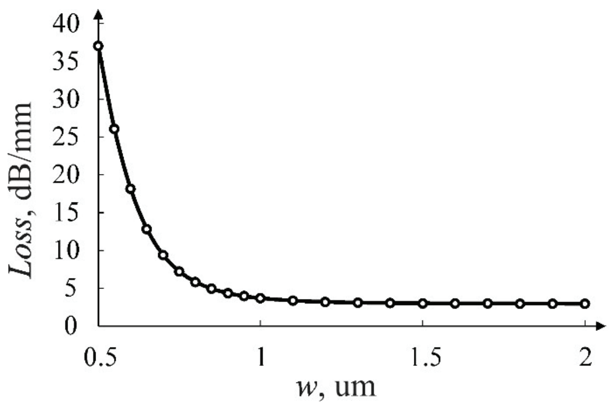

Figure 9 – Dependence of losses on the waveguide width for the 350-nm Si_3N_4 layer

For the silicon waveguide, the width and height were typical, and the minimal losses at a wavelength of 1550 nm were reached at their dimensions of 220 × 500 nm.

Optical error meter

The sensing element of the MOEM pressure sensor consisted of the membrane and the OMT represented by the directional coupler (Figure 10). The ports are designated in the figure.

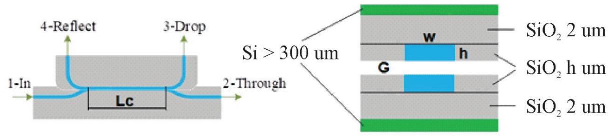

Figure 10 – Model of the directional coupler of the optical measuring transducer

Optical transmission coefficients of the directional coupler on the corresponding ports were determined as follows:

$$T_{through} = \frac{P_{through}}{P_{input}} = \cos^2\left(\frac{\pi \Delta n_{eff}}{\lambda} L_c\right); \quad (1)$$

$$T_{drop} = \frac{P_{drop}}{P_{input}} = \sin^2\left(\frac{\pi \Delta n_{eff}}{\lambda} L_c\right), \quad (2)$$

where $P_{thrpugh}$ is the output optical power at the «Through» port; P_{drop} is the output optical power at the «Drop» port; P_{input} is the input optical power at the «Input» port; λ is wavelength; L_c is the coupling length; Δn_{eff} is the difference between the effective refraction indices of the in-phase (n_{eff1}) and antiphase (n_{eff2}) harmonics of the carrier mode in the waveguides.

The coupling length L_c at which the optical power completely flowed from one waveguide into another one in the directional coupler was calculated as per equation (3) and corresponded to the maximum output power at the output of the «Drop» port:

$$L_c = \frac{\lambda}{2\Delta n_{eff}}. \quad (3)$$

Figures 11 and 12 demonstrate the distribution of the optical field in the coupled waveguides at different air gaps between them.

Following the figures, increased gap extended the coupling length at which the optical power completely flowed from one waveguide to another. For SOI waveguides, the air gap should be smaller. In the case of gaps identical to Si_3N_4, the critical coupling length should be larger.

The dependencies of effective refraction indices n_{eff1} and n_{eff2} on the gap are presented in Figures 13 and 14.

Therefore, according to equations (1) and (2), the alteration of the difference between the effective refraction indices would alter the optical power at the «Through» ad «Drop» ports. The most tech-

Devices and Methods of Measurements
2025;16(4):306–314
E.S. Barbin et al.

nologically rational approach is to use the optical power alteration induced by waveguide gap change at the «Through» port. The optical radiation from the «Drop» port should dissipate into the medium. The influence on the output signal at the «Through» port is minimal.

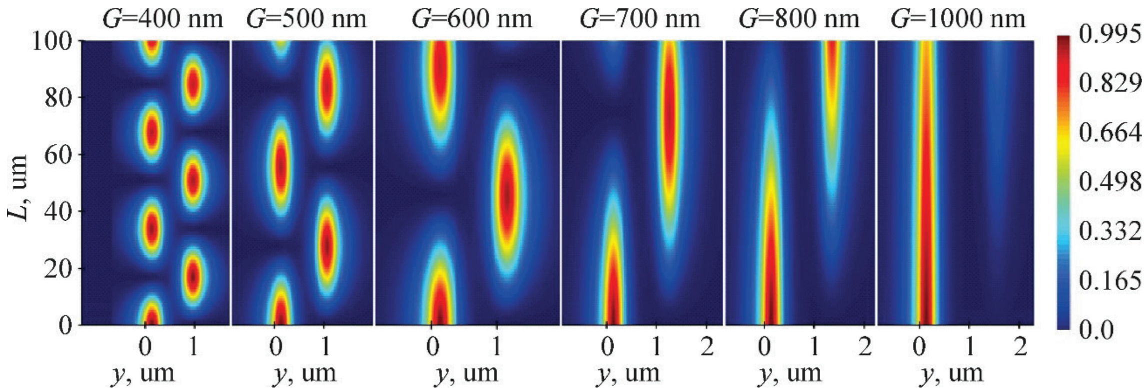

Figure 11 – Mode flow in Si_3N_4 waveguides (350×1400 nm)

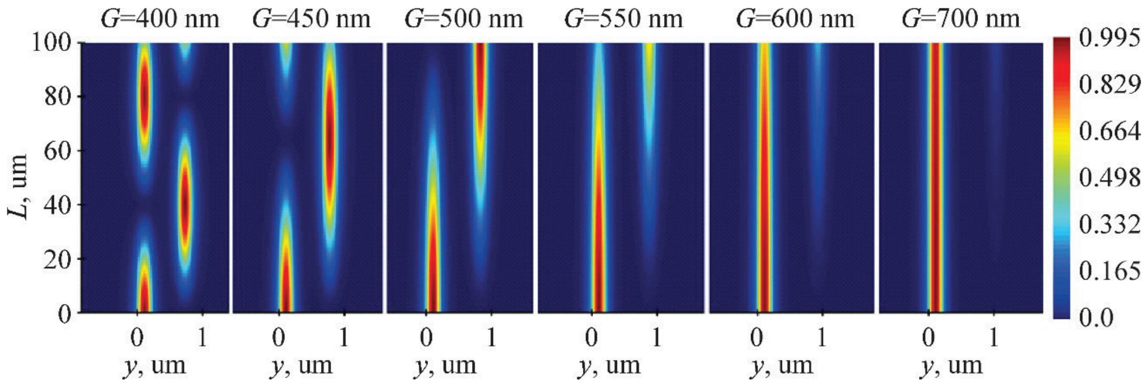

Figure 12 – Mode flow in SOI waveguides (220×500 nm)

According to the design concept of the MOEM pressure sensor, the primary interest for investigators is represented by the dependence of the optical power at the «Through» port. We scrutinized the dependencies of optical transmission coefficient «Tthrough» on coupling length L_c (Figures 15 and 16) and gap G (Figures 17 and 18) for Si_3N_4 waveguides (350×1400 nm) and SOI waveguides (220×500 nm). The top and bottom waveguides faced air on one side and silicon oxide on other three sides. Henceforth, T will denote optical transmission coefficient «Tthrough».

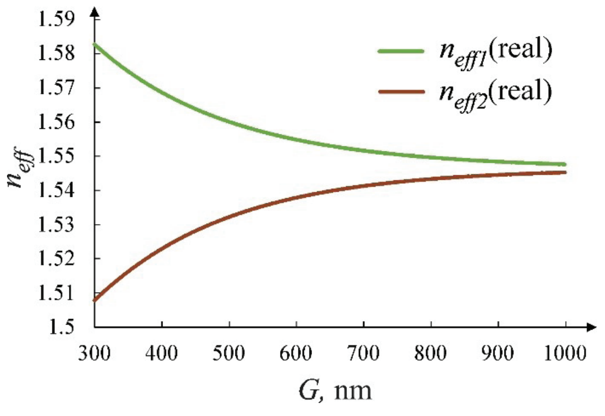

Figure 13 – Dependencies of effective refraction indices in Si_3N_4 waveguides (350×1400 nm)

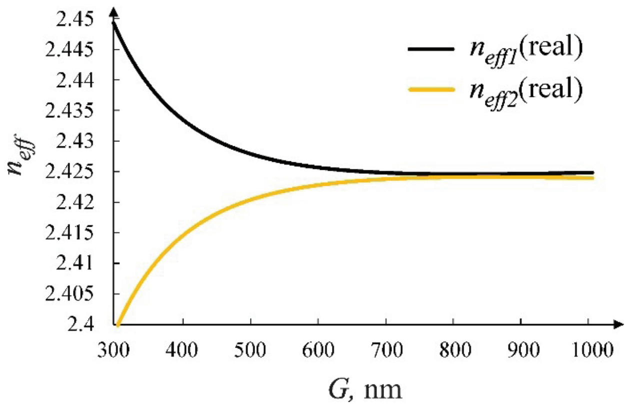

Figure 14 – Dependencies of effective refraction indices in SOI waveguides (220×500 nm)

Following technological reasons, decreased crystal area and optical path length of the photonic integrated circuit and reduced risks of movable and fixed parts of the MOEM structure, the studied coupling length was limited to 200 µm. The gaps under study were limited to 1000 nm.

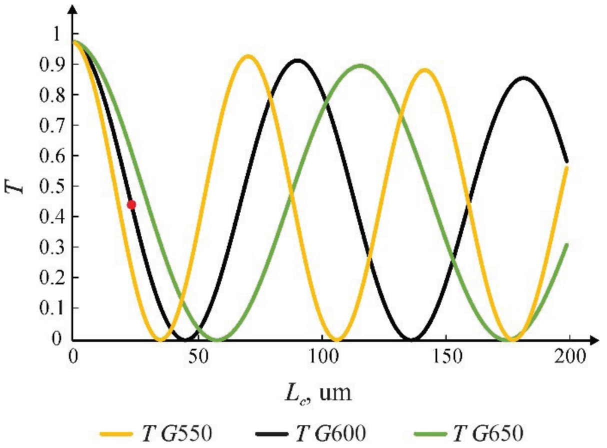

Figure 15 – Dependence of the transmission coefficient of the optical measuring transducer on the coupling length for the Si_3N_4 waveguide

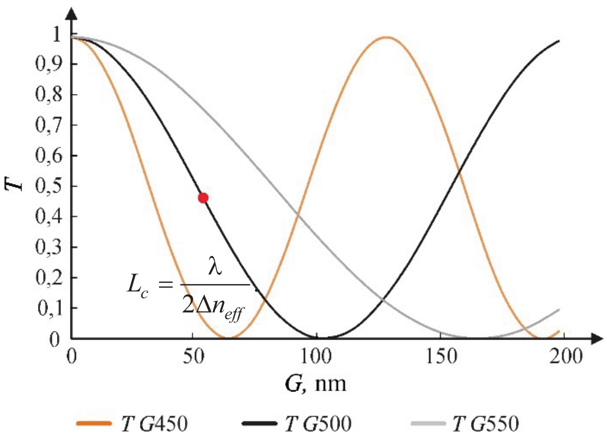

Figure 16 – Dependence of the transmission coefficient of the optical measuring transducer on the coupling length for the SOI waveguide

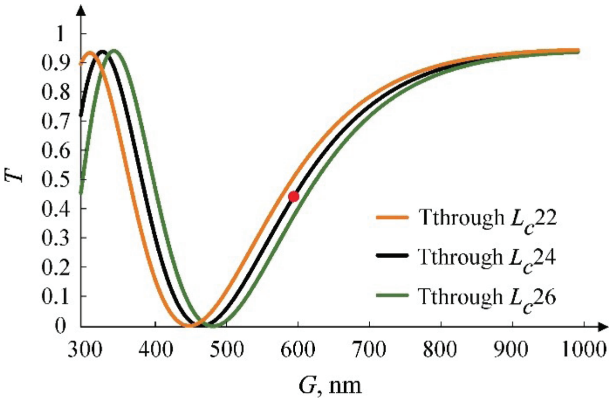

Figure 17 – Dependence of the transmission coefficient of the optical measuring transducer on the gap for the Si_3N_4 waveguide

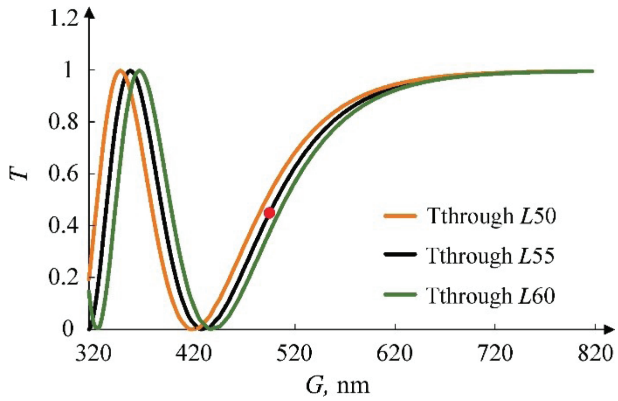

Figure 18 – Dependence of the transmission coefficient of the optical measuring transducer on the gap for the SOI waveguide

The plots 15–18 are the performance curves of the optical measuring transducer. The working range, where the OMT can measure membrane displacements proportional to acting pressure reached 500±80 nm for the SOI waveguide and 600±80 nm for the Si_3N_4 waveguide. The optical transmission coefficient ranged from 0 to 0.86 for the SOI waveguide and from 0.09 to 0.53 for the Si_3N_4 waveguide.

The transmission coefficient of the OMT was determined as:

$$K_0 = \frac{T_{onm}^{\max} - T_{onm}^{\min}}{G_{\max} - G_{\min}}, \tag{4}$$

where $T_{onm}^{\max}$, $T_{onm}^{\min}$ is the maximum and maximum optical power at the coupler output; $G_{\max}$, $G_{\min}$ – is the maximum and maximum gap between the waveguides.

Conclusion

A design concept of the sensing element of a micro-optoelectromechanical pressure sensor and its fabrication concept were developed. The pressure sensor is based on integrated optical waveguides and a directional coupler with constant air gap. The fixed waveguide is located on the fixed part, while the second waveguide is located on the membrane which bend value is proportional to the applied pressure.

The main characteristics were calculated: losses, dependencies of the transmission coefficients on the length and width of the waveguides, gap, coupling length. The performance curve was selected for two variants of fabrication: 350×1400-nm Si_3N_4-based waveguide and 220×50-nm SOI-based waveguide. Thus, the membrane deformation over the entire pressure range should not exceed 500±80 nm for SOI wafers and 600 ± 80 nm for Si_3N_4 wafers.

Acknowledgments

The results were obtained with the support of the Ministry of Science and Higher Education of the Russian Federation (theme No. FEWM-2024-0008).

References

1. Bhat KN, Nayak MM. MEMS Pressure Sensors-An Overview of Challenges in Technology and Packaging. Inst. Smart Struct. Syst. J. Isss J. Isss. 2012;1(1).

2. Barlian AA, Park W-T, Mallon JR, Rastegar AJ, Pruitt BL. Review: Semiconductor Piezoresistance for Microsystems. Proceedings of the IEEE, 2009;97(3):513-552. **DOI:** 10.1109/jproc.2009.201361

3. Kanekal D, Jindal SK. Investigation of MEMS Piezoresistive Pressure Sensor with a Freely Supported Rectangular Silicon Carbide Diaphragm as a Primary Sensing Element for Altitudinal Applications. Silicon 15, 2023;15(4):1947-1959.
DOI: 10.1007/s12633-022-02146-z

4. Kyoung-Ho Ha, Heeyong Huh, Zhengjie Li, Nanshu Lu. Soft Capacitive Pressure Sensors: Trends, Challenges, and Perspectives. ACS Nano. 2022;16(3):3442-3448.

5. Kim H, Jeong YG, Chun K. Improvement of the linearity of a capacitive pressure sensor using an interdigitated electrode structure. Sensors Actuators, A Phys. 1997;62(1–3):586-590.

6. Shahiri Tabarestani M. Analytical Analysis of Capacitive Pressure Sensor with Clamped Diaphragm. Int. J. Eng. 2013;26(3):297-302.

7. Jang M, Yun K-S. MEMS capacitive pressure sensor monolithically integrated with CMOS readout circuit by using post CMOS processes. Micro and Nano Systems Letters. 2017;5(1):4 p. **DOI:** 10.1186/s40486-016-0037-3

8. Boukabache A. [et al.]. Characterization and modelling of the mismatch of TCRs and their effects on the drift of the offset voltage of piezoresistive pressure sensors. Sensors Actuators, A Phys. 2000;84(3):292-296.
DOI: 10.1016/S0924-4247(00)00406-4

9. Belwanshi V. Analytical modeling to estimate the sensitivity of MEMS technology-based piezoresistive pressure sensor. J Comput Electron. 2021;(20):668-680.
DOI: 10.1007/s10825-020-01592-5

10. Tian B, Shang H, Zhao L [et al.]. Performance optimization of SiC piezoresistive pressure sensor through suitable piezoresistor design. Microsyst Technol. 2021;(27):3083-3093. **DOI:** 10.1007/s00542-020-05175-z

11. Kumar SS, Pant BD. Design principles and considerations for the "ideal" silicon piezoresistive pressure sensor: a focused review. Microsystem Technologies. 2014;20(7):1213-1247.
DOI: 10.1007/s00542-014-2215-7

12. Park S-H, Lee HB, Yeon SM, Park J, Lee NK. Flexible and Stretchable Piezoelectric Sensor with Thickness-Tunable Configuration of Electrospun Nanofiber Mat and Elastomeric Substrates. ACS Applied Materials & Interfaces. 2016;8(37): 24773-24781.
DOI: 10.1021/acsami.6b07833

13. Qian P, Yu Z, Yu J. [et al.]. A resonant high-pressure microsensor based on a composite pressure-sensitive mechanism of diaphragm bending and volume compression. Microsyst Nanoeng. 2024;10:38 p.
DOI: 10.1038/s41378-024-00667-8

14. Yulan Lu, Pengcheng Yan, Chao Xiang, Deyong Chen, Junbo Wang, Bo Xie and Jian Chen. A Resonant Pressure Microsensor with the Measurement Range of 1 MPa Based on Sensitivities Balanced Dual Resonators. Sensors. 2019;19(10):2272. **DOI:** 10.3390/s19102272

15. Yu J. [et al.]. A resonant high pressure sensor based on dual cavities design. IEEE 16th International Conference on Nano/Micro Engineered and Molecular Systems (NEMS). 2021;1725-1728 p.

16. Mitsuhashi T. [et al.]. A resonant pressure sensor with super high resolution and stability based on novel volume shrinkage method. in Transducers. 22nd International Conference on Solid-State Sensors, Actuators and Microsystems (Transducers) 2023. JAPAN.

17. Deyong Chen, Dafu Cui, Shanhong Xia Zheng Cui. Design and Modeling of a Silicon Nitride Beam Resonant Pressure Sensor for Temperature Compensation. Proceedings of the 2005 IEEE International Conference on Information Acquisition. 2005.

18. Xu MG, Geiger H, Dakin JP. Fibre grating pressure sensor with enhanced sensitivity using a glass-bubble housing. Electronics Letters. 1996;32(2).
DOI: 10.1049/el:19960022

19. Arkwright JW [et al.]. Fiber Optic Pressure Sensing Arrays for Monitoring Horizontal and Vertical Pressures Generated by Traveling Water Waves. IEEE Sensors Journal. 2014;14(8):2739-2742.
DOI: 10.1109/jsen.2014.2311806

20. Wang Y, Wang DN, Wang C, Hu T. Compressible fiber optic micro-Fabry-Pérot cavity with ultra-high pressure sensitivity. Optics Express. 2013;21(12):14084.
DOI: 10.1364/oe.21.014084

21. Yizheng Zhu, Anbo Wang. Miniature fiber-optic pressure sensor. IEEE Photonics Technology Letters. 2005;17(2):447-449. **DOI:** 10.1109/lpt.2004.839002

22. Cibula E, Donlagic D, Stropnik C. (n.d.). Miniature fiber optic pressure sensor for medical applications. Proceedings of IEEE Sensors. 2002;(1):711-714.
DOI: 10.1109/icsens. 2002/1037190/2010

23. Evgenii Barbin [et al.]. The Design, Modeling and Experimental Investigation of a Micro-G Microoptoelectromechanical Accelerometer with an Optical Tunneling Measuring Transducer. Sensors. 2024;24(3):765 p.
DOI: 10.3390/s24030765